Polymer Chemistry

PAPER

View Article Online
View Journal | View Issue

Cite this: *Polym. Chem.*, 2017, **8**, 3712

Advantages and limitations of diisocyanates in intramolecular collapse†

Feng Wang and Charles E. Diesendruck *

Received 26th April 2017,
Accepted 25th May 2017

DOI: 10.1039/c7py00712d

rsc.li/polymers

A comprehensive examination of the synthesis of single chain polymer nanoparticles (SCPNs) from a co-polymer of methyl acrylate (MA) and 2-hydroxyethyl acrylate (HEA) *via* the intra-chain urethane formation by using hexamethylene diisocyanate (HDI) as a cross-linker is described. By introducing model urethane, urea, and amine compounds, the resulting SCPNs were carefully characterized by NMR, DSC, IR and GPC. In addition to the advantages of using cheap and accessible commercially available materials, the effects of the long reaction time under high dilution or harsher heating conditions on the cross-linking chemistry are studied, providing clear limitations on the use of this chemistry for intra-chain collapse.

Introduction

In recent years, there has been growing interest in the fabrication of devices and soft nano-objects based on the manipulation of polymer nanoparticles.[1–8] Among the various synthetic approaches for organic nanoparticles, the preparation of single chain polymer nanoparticles (SCPNs), obtained from the intramolecular collapse of polymer chains into very small particles (5–20 nm),[1,9–14] has been particularly eye-catching. SCPNs, though simple in concept, exhibit fairly complicated behaviour[15–19] and present promising prospects in various applications, such as nanomedicine,[20–22] catalysis,[12,14,22–26] sensing,[27] mimicry of folded proteins,[28–30] and more.

While there are a plethora of synthetic approaches towards SCPNs, the chemistry used for the main chain and collapse is crucial for developing applications, as they define the practicality of SCPN synthesis, as well as properties.[1,11] Chain collapse is induced by intramolecular bond formation (covalent,[31,32] dynamic covalent[33–35] or non-covalent[36–38]) in conventional linear polymeric backbones containing pendant reactive groups. Thanks to the dramatic advances in controlled radical polymerization (CRP)[39–43] and post-polymerization modification reactions,[44–46] SCPN studies are booming, with a variety of highly efficient cross-linking chemistries being applied in the synthesis of new SCPNs in different shapes[47–51] and scales.[52–56]

Among the different tested chemistries, commercially available or easily accessible monomers and cross-linkers that react cleanly in high yield present clear advantages. Consequently, click chemistry,[20,50,57–60] radical coupling,[9,61] benzocyclobutane dimerization,[31,62–64] Bergmann cyclization,[65,66] Diels–Alder ligation,[67,68] *etc.*, are frequently employed as these reactions are highly efficient and produce no side products.

Isocyanates are well-known to react efficiently with thiols, amines and alcohols under mild conditions without side products, and are therefore widely used in polymer chemistry.[69–72] The preparation of SCPNs from isocyanate containing acrylate monomers has been reported,[73] yet extreme caution is needed during polymerization and storage, given the sensitivity and reactivity of isocyanate side-chains. The alternative to that is to prepare polymers with primary amines, thiols or alcohol nucleophiles as side chains. While polymerization of monomers with thiol or primary amine side-chains is tricky, as they interfere with the propagating radicals,[39] hydroxide groups are compatible with the CRP protocols, and do not require protection and deprotection reactions, reducing the number of steps. Monomers, such as 2-hydroxyethyl acrylate (HEA) and 2-hydroxyethyl methacrylate (HEMA), are commercially available, convenient to handle and different CRP protocols have been put forward for their polymerization or copolymerization.[74–77] Additionally, SCPNs from PHEA or PHEMA based polymers and copolymers which are biocompatible[78,79] have the potential to deliver covalently attached small molecules such as drugs or dyes, given that SCPNs can enter cells.[22,26]

However, only during the preparation of this manuscript the first single chain collapse from the reaction of HEA units with aromatic diisocyanates has been reported, where it was used to make a complicated SCPN structure.[80] However, a comprehensive study of this typically simple reaction, such as the detailed chemistry and structure of the cross-links, chain collapse kinetics and the effect of cross-linking on the properties of the isolated nanoparticles, is required, given the special conditions required for intramolecular chain collapse.

Schulich Faculty of Chemistry and Russell-Berrie Nanotechnology Institute, Technion – Israel Institute of Technology, Haifa, 32000, Israel. E-mail: charles@technion.ac.il

†Electronic supplementary information (ESI) available. See DOI: 10.1039/c7py00712d

Herein, the P(MA-*co*-HEA) copolymer was prepared and a systematic study on the synthesis of SCPNs from P(MA-*co*-HEA) *via* the intra-chain urethane formation by using hexamethylene diisocyanate (HDI) as a cross-linker is described. In addition, model small molecules (urethane, urea and amine) were prepared to thoroughly uncover the precise chemical composition of the resulting SCPNs. The effects of temperature on the kinetics of chain collapse and the amount of HDI on the properties of resulting SCPNs were investigated. The advantages and limitations of this kind of reaction for intra-chain collapse are also discussed.

Experimental

Materials

Methyl acrylate (MA) and 2-hydroxyethyl acrylate (HEA) were purified by filtration through basic alumina to remove the inhibitor, after which they were kept at 4 °C under argon. Tetrahydrofuran (THF) and dimethylsulfoxide (DMSO) were purified by the method developed by Williams *et al.*[81] All other chemicals including, methyl α-bromoisobutyrate (MBiB), hexamethylene diisocyanate, tris(2-dimethylaminoethyl)amine (Me_6TREN) and dibutyltin dilaurate (DBTDL) were obtained from commercial sources and used as received. All reactions were carried out in heat-gun-dried glassware under an argon atmosphere using the standard Schlenk techniques.

Characterization

All ^{1}H and ^{13}C NMR spectra were recorded using an Avance 300 MHz Bruker spectrometer at the Technion NMR facilities. Proton chemical shifts are expressed in parts per million (ppm, δ scale) and are referenced to tetramethylsilane ($(CH_3)_4Si$, 0.00 ppm) or residual protium in the solvent (DMSO-d_5, 2.50 ppm).

GPC measurements were performed in THF at a flow rate of 1 mL min^{-1} at 30 °C, using a Thermo HPLC system consisting of a Dionex Ultimate 3000 isocratic pump, four in line TSKgel G4000HHR columns and a series of five detectors, Dionex DAD-3000 UV-VIS detector, a Wyatt Dawn Heleos II 8 multi-angle light scattering, including DLS (Wyatt QELS), refractometer (Wyatt Optilab-rEX) and viscometer (Wyatt Viscostar II). Data analysis was performed using ASTRA 6 software from Wyatt. The d*n*/d*c* used for P(MA-*co*-HEA) was 0.068 mL g^{-1}. Attenuated total reflection-Fourier transform infrared (ATR-FTIR) spectra were recorded on a JASCO 3600 FTIR spectrometer at room temperature. Glass transitions of all samples were measured on a Mettler Toledo Differential Scanning Calorimeter (DSC) under a continuous flow of nitrogen. In all tests, a scan rate of 10 K min^{-1} was used in the temperature range of −60 °C to 100 °C for the three heating and cooling cycles. The T_g values were determined from the third cycle.

Synthesis of P(MA-*co*-HEA) linear precursor

The copolymer was synthesized through a single electron transfer living radical polymerization (SET-LRP).[77,82] MA (1.0 mL, 11.10 mmol), HEA (0.22 mL, 1.96 mmol), DMSO (2 mL), initiator (MBiB, 1.2 μL, 9.47 μmol), copper wire (diam. 0.5 mm, 2 cm length), and ligand (Me_6TREN, 1.3 μL, 4.73 μmol) were added into a 10 mL Schlenk flask under argon. The flask was immediately sealed and three freeze–pump–thaw cycles were applied to remove dissolved oxygen and then the flask was backfilled with argon and allowed to be stirred in a water bath for 2 h at room temperature. The polymerization was quenched by exposure to air. The solution was diluted with 10 mL CH_2Cl_2, filtered through basic alumina before concentration in vacuum, precipitation in diethyl ether, filtration and drying under vacuum. The yield was 79.0%.

Synthesis of single chain polymer nanoparticles

A typical intramolecular cross-linking procedure is as follows ($SCPNs_{15}$): P(MA-*co*-HEA) (100 mg, *n*(OH) = 0.173 mmol, 15.7 mol% in copolymer) was dissolved in dry THF (85 mL). Argon was bubbled for 15 min before a diluted solution of HDI (14.0 μL, 0.086 mmol, aiming at 15% crosslink density) and DBTDL (10.0 μL, 16.6 μmol) in dry THF (15 mL) were added dropwise. The progression of the reaction was followed by GPC measurements. After completion, excess *n*-butylamine was added to quench unreacted isocyanate groups. Subsequently, the reaction mixture was evaporated under reduced pressure and the product was precipitated in diethyl ether, filtered and dried under high vacuum. The yield was 94.5%.

Results and discussion

The syntheses of the polymers used in this study are shown in Scheme 1. Firstly, the P(MA-*co*-HEA) linear precursor was prepared *via* SET-LRP at room temperature. Recently, SET-LRP has been reported as an efficient approach to homopolymerize the protic monomer HEA under mild conditions providing PHEA with a narrow polydispersity index (PDI) and experimental M_n values that correlate well with their theoretical values.[77] Herein, a linear P(MA-*co*-HEA) was prepared in DMSO with M_n = 99.0 kDa and PDI = 1.20. The mole fraction of the HEA units in the copolymer was determined to be 15.7 mol% using ^{1}H-NMR spectroscopy.

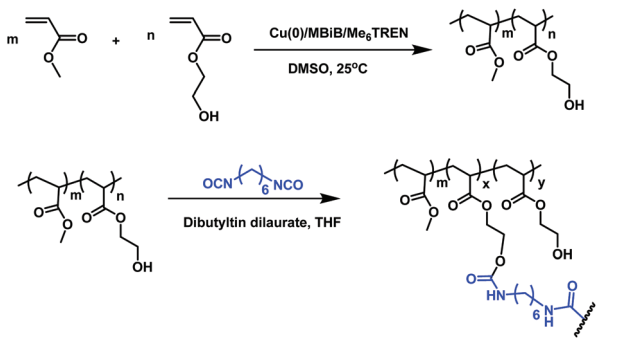

Scheme 1 Synthesis of the polymers used in this study.

Intramolecular collapse was tested initially by employing HDI as a cross-linker in view of the efficient reaction of isocyanates with alcohols[83] under tin(II) or tertiary amine catalysis, largely employed for polyurethane synthesis.[70,84] In our hands, the best reaction conditions were to dilute the P(MA-*co*-HEA) linear precursor to 1 mg mL^{-1} (*ca.* 10^{-5} M) in THF followed by addition of HDI and DBTDL in THF.

As a model reaction, we added HDI equivalent to 15 mol% cross-link density. Chain collapse was implemented at room temperature (labelled as $SCPNs_{15}$ (20 °C)), and monitored *via* GPC analysis. The GPC, equipped with multi-angle light scattering (MALS), a viscometer and refractive index (RI) detectors, enables following the change in the absolute molecular weight as well as the hydrodynamic radius concomitantly.

As the reaction progresses, an unambiguous increase in the retention time is observed (Fig. 1a), pointing to a reduction in the hydrodynamic volume. In addition, the average molecular weight increases gradually, as expected for the reaction with an external cross-linker, while a significant drop in the intrinsic viscosity and hydrodynamic radii is also observed (see the ESI, Table S1†), confirming that the change in the retention time is indeed due to chain collapse. After 48 h, almost no discernible increase in the retention time implied that the reaction became too sluggish or completed. Unfortunately, isolation of the nanoparticles by drying under vacuum resulted in gelation of the sample, probably due to the presence of unreacted isocyanate and hydroxyl groups. To overcome this undesired intermolecular cross-linking, the reaction was repeated and excess *n*-butylamine was added at the end to cap unreacted isocyanates. To our satisfaction, this time the resulting material could be readily redissolved in THF. Fig. 1b shows an overlay of the MALS and RI detector signals for the isolated $SCPNs_{15}$ (20 °C). No shoulders or peaks at lower retention times are observed in these detectors indicating the absence of undesired multi-chain aggregates.

In an attempt to accelerate the synthesis of these SCPNs, we tested the procedure at elevated temperatures: 30 °C, 40 °C, and 60 °C. Taking $SCPNs_{15}$ (60 °C) for example, as observed in Fig. 2a, the intramolecular cross-linking reaction was completed much faster than at room temperature, 3 h (Fig. 2a) *versus* 32 h. The reaction kinetics could be measured by monitoring the hydrodynamic radius (R_h) values as a function of reaction time.[28] The pseudo-first-order kinetics plot disclosed that the apparent rate constant of the intra-chain folding reaction increases with elevation of temperature (Fig. 2b). An activation barrier (E_a) of 53.0 kJ mol^{-1} was calculated from the kinetic data using an Arrhenius plot (see Fig. S5 in the ESI†).

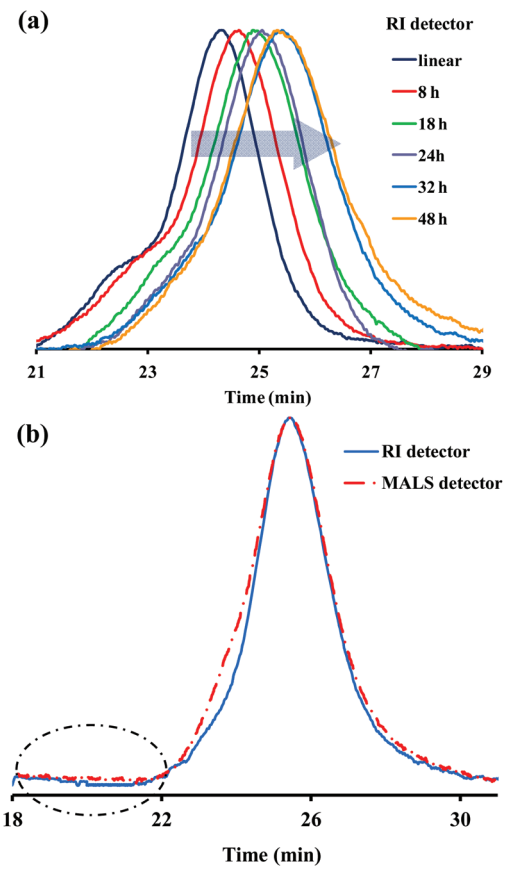

Fig. 1 (a) Evolution of SEC traces of the $SCPNs_{15}$ (20 °C) sample during chain folding. Aliquots were removed at the specified time. (b) GPC traces of the isolated $SCPNs_{15}$ (20 °C) sample.

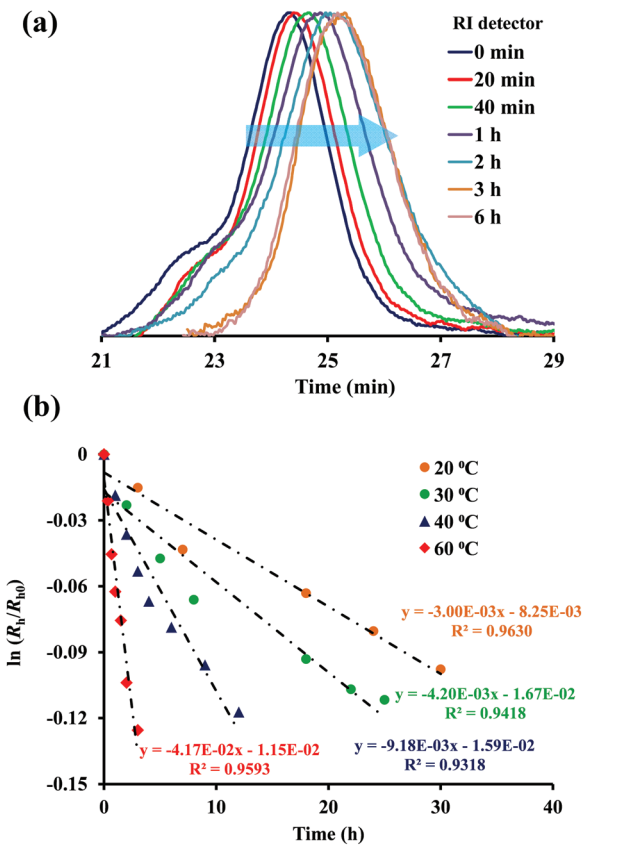

Fig. 2 (a) Evolution of GPC traces of the $SCPNs_{15}$ (60 °C) sample during chain folding. Aliquots were removed at the specified time. (b) Pseudo-first-order kinetics plots corresponding to the folding procedure at 20 °C, 30 °C, 40 °C and 60 °C, respectively.

Direct evidence of urethane formation between the hydroxyl group in the HEA unit and isocyanate moieties was obtained by ATR-FTIR spectroscopy (Fig. 3). While the isocyanate peak at 2280 cm^{-1} is not observed in the isolated polymers, new peaks at 1624 cm^{-1}, 1581 cm^{-1}, 1540 cm^{-1} and 3350 cm^{-1} clearly emerge after the reaction (Fig. 3A). To identify the new carbonyl peaks, model urethane and urea compounds were prepared through reactions of HDI with ethanol and *n*-butylamine, respectively. In comparison with the IR spectra of the model urea and urethane compound (Fig. 3B), the peaks at 1624 cm^{-1} and 1581 cm^{-1} in the SCPN sample were ascribed to the formation of urea groups while the peak at 1540 cm^{-1} was assigned to the formation of the urethane group (an additional urethane peak at 1718 cm^{-1} overlaps the ester peak of MA and the HEA repeating unit).[71]

In addition to the expected urethane peaks, significant urea peaks are also clearly observed in the IR spectra of isolated SCPNs. Several possible reactions can explain the presence of both urea and urethane groups during the chain collapse process (Scheme 2): (I) the expected intra-chain cross-link by reaction between HDI and HEA units, forming the urethane group; (II) the reaction between isocyanate and *n*-butylamine which is used to cap unreacted isocyanates, introducing a urea group; (III) the hydrolysis of isocyanates, resulting in a primary amine, even though dry solvents and reagents were used; (IV) and (V) the resulting primary amine in (III) reacts with isocyanates (HDI, IV or side-group V) to form a urea unit.

To uncover evidence of these possible reactions, systematic ^{1}H NMR and ^{13}C NMR studies were conducted. Firstly, ^{13}C NMR spectroscopy investigation was implemented. As in IR, we compared the ^{13}C NMR spectra of $SCPNs_{15}$ with that of the linear precursor and model urethane and urea compounds (Fig. 4). ^{13}C NMR revealed the appearance of new carbonyl signals at 155.6 (r) and 158.4 (s) ppm arising from urethane and urea groups respectively, reinforcing the observations from the IR spectra. A comparison with model urea and urethane compounds indicates the absence of a terminal methyl group in $SCPNs_{15}$ (20 °C) and $SCPNs_{15}$ (60 °C), demonstrating that reaction (II) is minor and not the source of the urea groups. Therefore, urea must be coming from the reaction with water followed by a subsequent reaction with an additional isocyanate (IV or V).

To verify if terminal amines are present in the isolated SCPNs, we looked for N–H peaks or CH_2NH_2 in the ^{1}H NMR. Firstly, we assigned these signals in the ^{1}H NMR spectrum of model hexylamine. Unfortunately, the $-NH_2$ protons overlap with additional aliphatic protons, and the signal of $-CH_2NH_2$ overlaps with DMSO-d_5 (Fig. 5A). To resolve this, one drop of

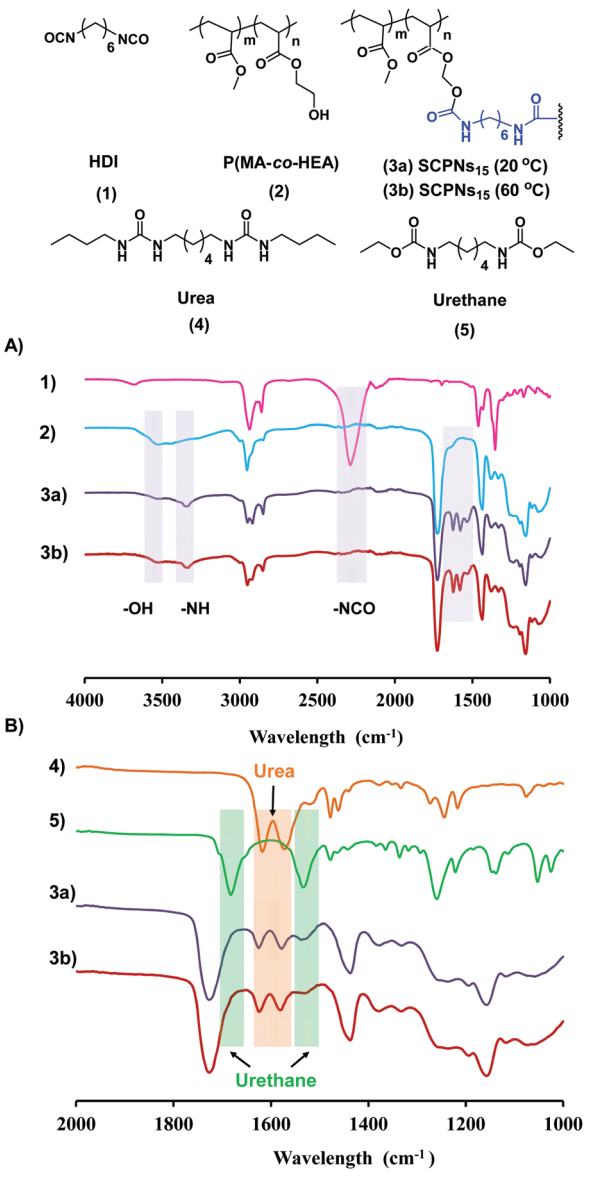

Fig. 3 (A) IR spectra of HDI, P(MA-*co*-HEA), $SCPNs_{15}$ (20 °C) and $SCPNs_{15}$ (60 °C) samples. (B) IR spectra of model urea compound, model urethane compound, $SCPNs_{15}$ (20 °C) and $SCPNs_{15}$ (60 °C) samples.

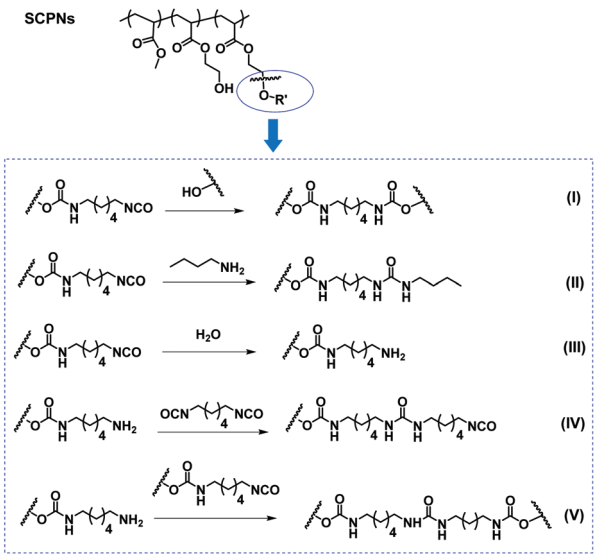

Scheme 2 Possible reactions during chain collapse.

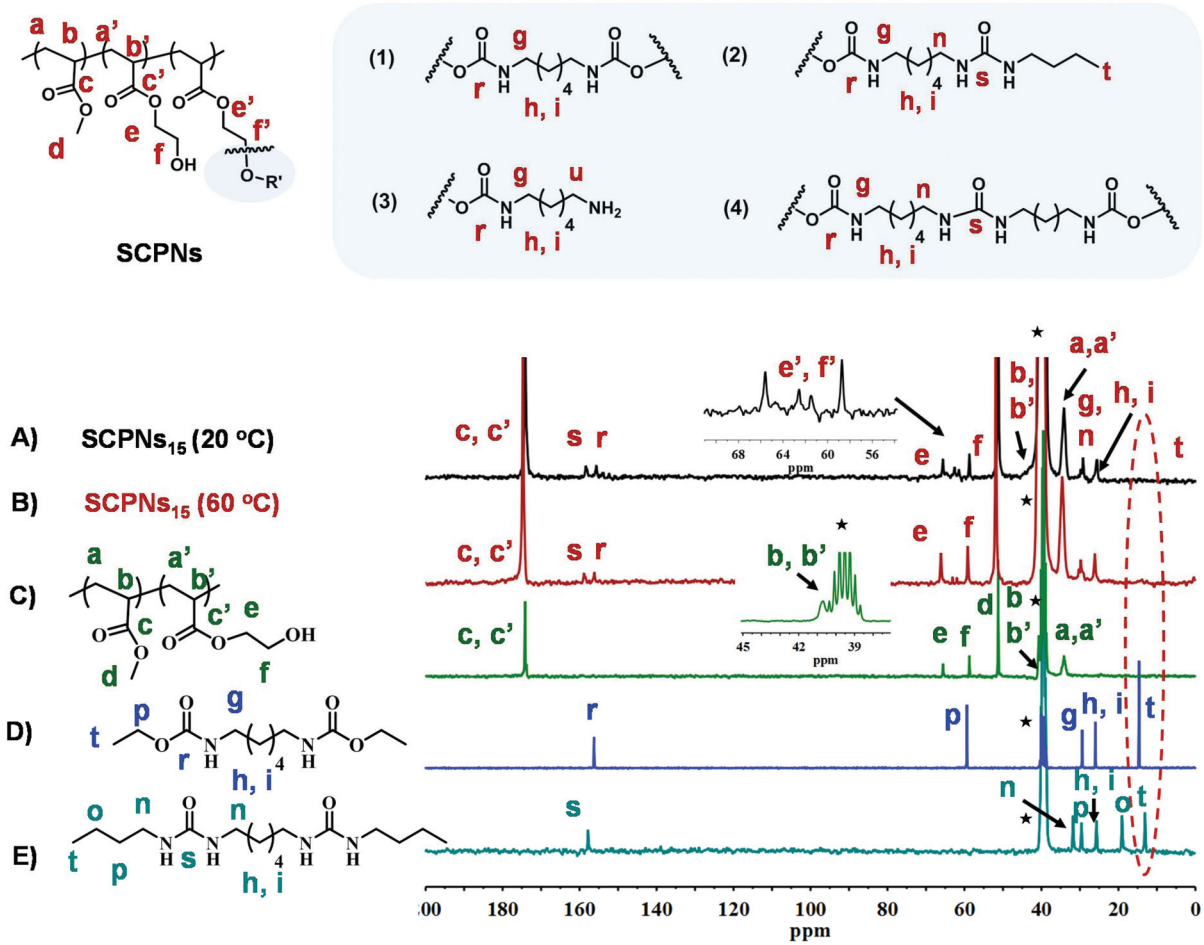

Fig. 4 ^{13}C NMR spectra of (A) $SCPNs_{15}$ (20 °C), (B) $SCPNs_{15}$ (60 °C), (C) P(MA-*co*-HEA), (D) model urethane compound, and (E) model urea compound, ⋆DMSO-d_5.

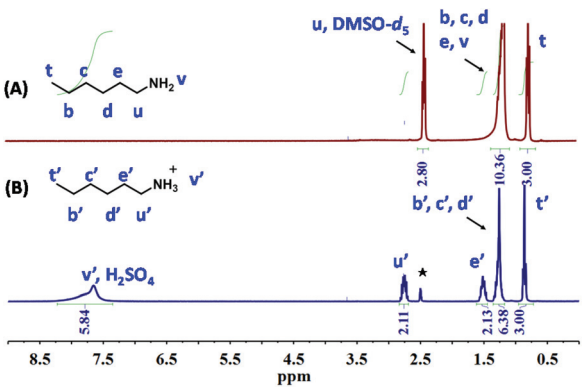

Fig. 5 (A) ^{1}H NMR spectrum of hexylamine in DMSO-d_6. (B) ^{1}H NMR spectrum of hexylamine upon addition of one drop of H_2SO_4 into DMSO-d_6. ⋆DMSO-d_5.

concentrated sulfuric acid (H_2SO_4) was added, shifting both ammonium and –C***H***$_2$NH$_3^+$ protons to lower fields (7.64 and 2.77 ppm respectively, Fig. 5B), providing in both cases isolated peaks. Similarly, H_2SO_4 was added to model urea and urethane compounds (ESI, Fig. S7 and S8†). As in hexylamine, the acidic N***H***COO– (k, urethane) and –N***H***CON***H***– (m, urea) protons shift upon addition of the acid, but methylene protons in –C***H***$_2$NHCOO– (g) and –C***H***$_2$NHCONHC***H***$_2$– (n) remain mostly unchanged (see the ESI†), as opposed to the –C***H***$_2$NH$_2$ (u, Fig. 5) in hexylamine.

Based on this distinction, we analyzed the ^{1}H NMR spectra of $SCPNs_{15}$ (20 °C) and the same spectra upon acid addition. The ^{1}H NMR results revealed the expected shifts for –N***H***COO– (k, urethane group, Fig. 6) and –N***H***CON***H***– (m, urea group, Fig. 6). If terminal amines are present, upon addition of acid, –C***H***$_2$NH$_3^+$ (u′, Fig. 5B) should be formed shifting the methylene protons to *ca.* 2.8 ppm, overlapping with the methylene α to urea or urethane (g′, n′, Fig. 6B), leading to a relative increase in their integration. However, the relative integration of these protons (g, n, Fig. 6A) remains unchanged upon acid addition, indicating that if –C***H***$_2$NH$_2$ (u in (3), Fig. 6A) is present, it is too small for detection. In other words, no significant amount of primary amine is present in $SCPNs_{15}$ (20 °C). This was rather expected, as primary amines react with iso-

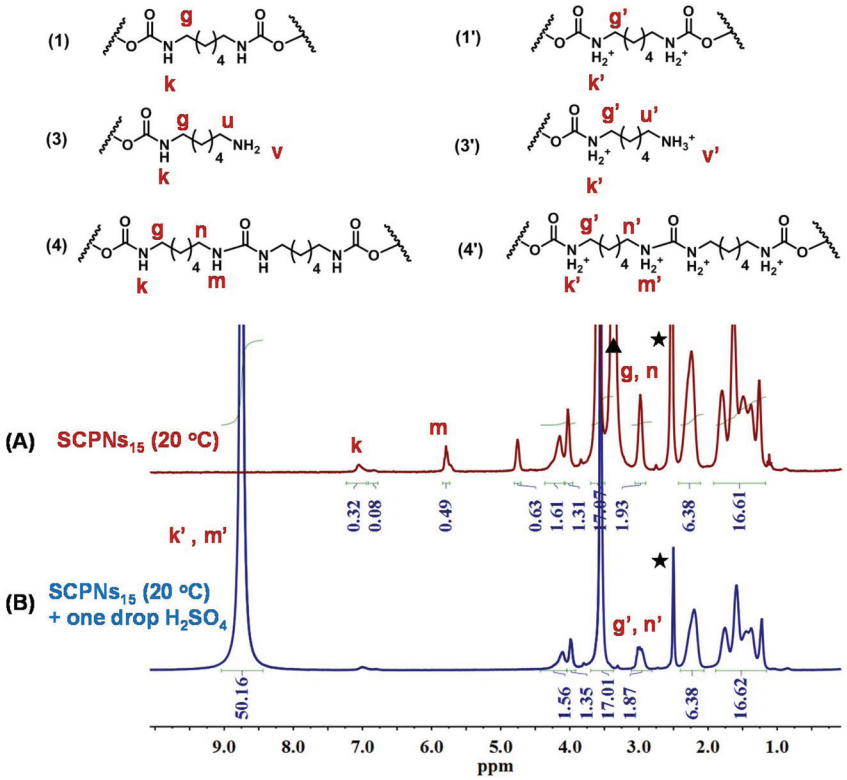

Fig. 6 (A) ^{1}H NMR spectrum SCPNs$_{15}$ (20 °C). (B) ^{1}H NMR spectrum of SCPNs$_{15}$ (20 °C) upon addition of one drop of H_2SO_4 into DMSO-d_6, *DMSO-d_5.

cyanates significantly faster than alcohols. The ^{1}H NMR spectra of SCPNs$_{15}$ (60 °C) with and without addition of acid (ESI, Fig. S9†) showed similar results, further confirming that urea groups arise from reaction with water (III) followed by reactions (IV) and (V), and no significant free amine groups remain. The assignment of every proton signal in the ^{1}H NMR of SCPNs is shown in Fig. 7.

Using the ratio between hydrogens e′, f′ to b, b′ the precise crosslink density can be calculated. For SCPNs$_{15}$ (20 °C), the cross-link density is 6.3 mol% (with a molar ratio of urethane/urea of 56.7/43.3); while for sample SCPNs$_{15}$ (60 °C), the cross-link density is about 4.4 mol%, and the molar ratio of urethane/urea is 44.4/55.6. These key measurements indicate that part of the HDI is consumed by the reaction with undesired primary amines reducing the cross-link density and lengthening cross-linkers. Although the reaction of alcohols and isocyanates under tin(II) catalysis is well documented and largely applied for polyurethane synthesis, under high dilution conditions, the selectivity is decayed due to what seems inevitable reaction with water, even if purified solvent and Schlenk conditions are used. Importantly, our urethane model compound was prepared using similar solvents and Schlenk conditions, but no urea is apparent.

Finally, we tested how the cross-link density is affected by the amount of added HDI, generating SCPNs with different sizes from the same linear P(MA-*co*-HEA) precursor. Accordingly, we added the amount of HDI according to the desired crosslink density of 1 mol%, 3 mol%, 5 mol%, 10 mol% and 15 mol% (labelled as SCPNs$_1$, SCPNs$_3$, SCPNs$_5$, SCPNs$_{10}$ and SCPNs$_{15}$ respectively) and performed the reac-

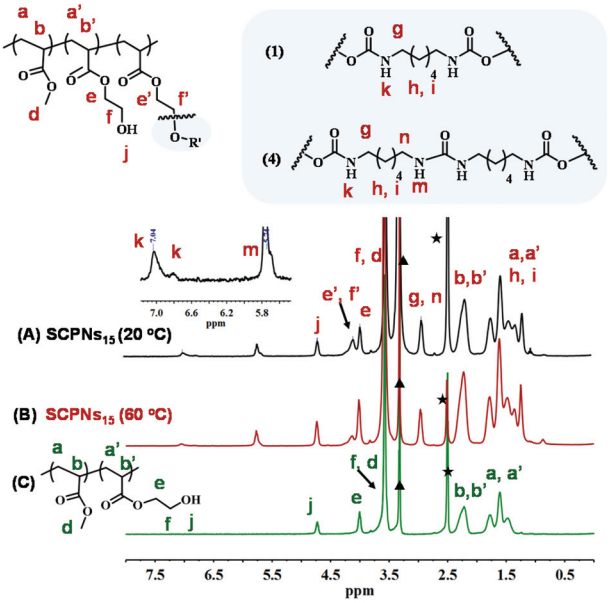

Fig. 7 ^{1}H NMR spectra of SCPNs$_{15}$ (20 °C), SCPNs$_{15}$ (60 °C) and P(MA-*co*-HEA) in DMSO-d_6.

tions at 60 °C. The desired cross-link density is calculated based on the molar ratio of reacted HEA units. The actual crosslink density for each sample was determined by ^{1}H NMR (ESI, Fig. S9–S13 and eqn (2)†) and is shown in Table 1. GPC analysis (Table 1 and Fig. 8) revealed a visible change in the hydrodynamic volume even for a low cross-link density (0.47 mol%). As expected, increasing the amount of HDI generates more compact structures with lower hydrodynamic radii and intrinsic viscosities, albeit there is no good control of the actual cross-link density or cross-linker length.

Changing the cross-link density also influences the segmental mobility of the chains, affecting their glass transition temperature (T_g).[85] Indeed, compared to the linear copolymer, the T_g values of SCPNs increase gradually from an initial value of 13.5 °C (linear polymer) up to 21.9 °C for SCPNs$_{15}$ (Fig. 9).

Table 1 Characteristics of P(MA-*co*-HEA) and corresponding SCPNs[a]

Sample	M_n[b] (kDa)	PDI[b]	[η][b] (mL g^{-1})	R_h[b] (nm)	Cross-link density[c] (mol%)	T_g[d] (°C)
P(MA-*co*-HEA)	99.0	1.20	37.3	8.35		13.5
SCPNs$_1$	99.8	1.15	36.5	8.30	0.47	13.9
SCPNs$_3$	104.0	1.13	33.7	8.07	1.88	15.7
SCPNs$_5$	107.8	1.12	30.1	7.80	2.35	16.7
SCPNs$_{10}$	111.9	1.12	28.2	7.62	3.08	21.2
SCPNs$_{15}$	120.8	1.12	25.5	7.50	4.41	21.9

[a] Reaction temperature: 60 °C. [b] Determined by GPC in THF at 30 °C. [c] Determined by ^{1}H NMR. [d] Determined by DSC.

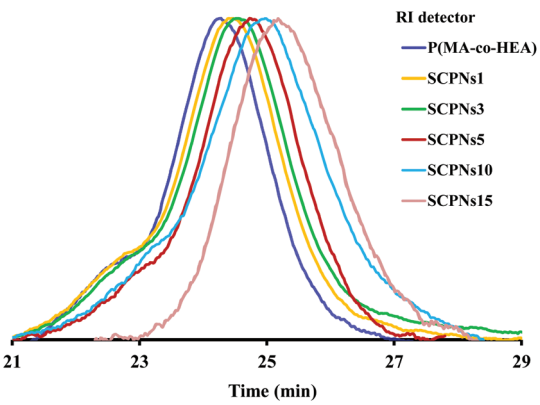

Fig. 8 GPC traces of SCPNs samples aiming at different cross-link densities.

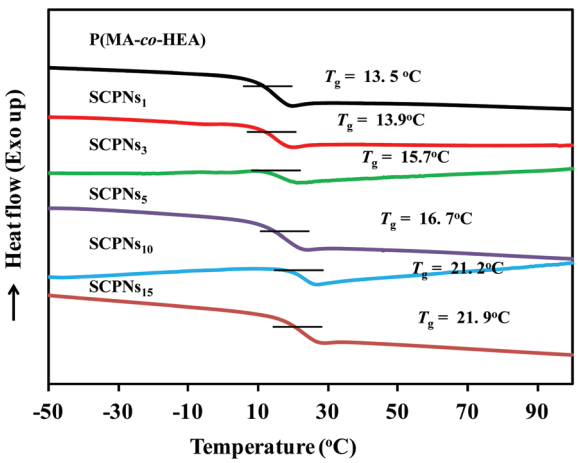

Fig. 9 DSC curves (second heating scan) for P(MA-*co*-HEA) and the corresponding nanoparticles.

Conclusions

In summary, we studied the kinetics and selectivity of the intra-chain collapse of a model polyalcohol made from cheap and widely available monomers. We've shown that increasing reaction temperature can lead to significant improvement in the time required to complete these high-dilution reactions, leading to SCPNs with different sizes, T_gs and rigidities in only a few hours. The use of widely available monomers and cross-linkers with fast reaction time provides easy access to large amounts of SCPNs. However, we've shown that the selectivity of diisocyanate chemistry towards formation of urethanes is partial at best, and a significant part of the HDI is consumed through the formation of urea, increasing the length of the cross-linker but reducing the actual cross-link density. The mechanism for urea formation was studied using NMR, and was shown to be mainly a consequence of water impurity and not due to amine capping. Yet, even when working under dry conditions – solvent drying and Schlenk techniques – these reactions could not be avoided. With all the advantages and disadvantages presented, this approach still presents a simple route to SCPNs which can be made water soluble and further functionalized with drug molecules for potential drug-delivery applications.

Acknowledgements

This material is based upon work supported by the Israel Science Foundation (grant no. 920/15). The authors thank Chemada Fine Chemicals for the kind donation of methyl α-bromoisobutyrate. FW is grateful to the GTIIT for a post-doctoral fellowship.

References

1 M. Gonzalez-Burgos, A. Latorre-Sanchez and J. A. Pomposo, *Chem. Soc. Rev.*, 2015, **44**, 6122–6142.
2 K. Landfester, *Adv. Mater.*, 2001, **13**, 765–768.
3 A. Monguzzi, M. Frigoli, C. Larpent, R. Tubino and F. Meinardi, *Adv. Funct. Mater.*, 2012, **22**, 139–143.
4 O. Rheingans, N. Hugenberg, J. R. Harris, K. Fischer and M. Maskos, *Macromolecules*, 2000, **33**, 4780–4790.
5 J. B. Matson and R. H. Grubbs, *J. Am. Chem. Soc.*, 2008, **130**, 6731–6733.

6 S. H. Medina and M. E. H. El-Sayed, *Chem. Rev.*, 2009, **109**, 3141–3157.
7 O. Altintas and C. Barner-Kowollik, *Macromol. Rapid Commun.*, 2012, **33**, 958–971.
8 C. K. Lyon, A. Prasher, A. M. Hanlon, B. T. Tuten, C. A. Tooley, P. G. Frank and E. B. Berda, *Polym. Chem.*, 2015, **6**, 181–197.
9 D. Mecerreyes, V. Lee, C. J. Hawker, J. L. Hedrick, A. Wursch, W. Volksen, T. Magbitang, E. Huang and R. D. Miller, *Adv. Mater.*, 2001, **13**, 204–208.
10 O. Altintas and C. Barner-Kowollik, *Macromol. Rapid Commun.*, 2016, **37**, 29–46.
11 S. Mavila, O. Eivgi, I. Berkovich and N. G. Lemcoff, *Chem. Rev.*, 2016, **116**, 878–961.
12 S. Mavila, C. E. Diesendruck, S. Linde, L. Amir, R. Shikler and N. G. Lemcoff, *Angew. Chem., Int. Ed.*, 2013, **52**, 5767–5770.
13 J. A. Kaitz, C. M. Possanza, Y. Song, C. E. Diesendruck, A. J. H. Spiering, E. W. Meijer and J. S. Moore, *Polym. Chem.*, 2014, **5**, 3788–3794.
14 I. Berkovich, S. Mavila, O. Iliashevsky, S. Kozuch and N. G. Lemcoff, *Chem. Sci.*, 2016, **7**, 1773–1778.
15 M. E. Mackay, T. T. Dao, A. Tuteja, D. L. Ho, B. Van Horn, H.-C. Kim and C. J. Hawker, *Nat. Mater.*, 2003, **2**, 762–766.
16 J. A. Pomposo, I. Perez-Baena, F. Lo Verso, A. J. Moreno, A. Arbe and J. Colmenero, *ACS Macro Lett.*, 2014, **3**, 767–772.
17 L. G. Schultz, Y. Zhao and S. C. Zimmerman, *Angew. Chem., Int. Ed.*, 2001, **40**, 1962–1966.
18 N. G. Lemcoff, T. A. Spurlin, A. A. Gewirth, S. C. Zimmerman, J. B. Beil, S. L. Elmer and H. G. Vandeveer, *J. Am. Chem. Soc.*, 2004, **126**, 11420–11421.
19 A. Levy, F. Wang, A. Lang, O. Galant and C. E. Diesendruck, *Angew. Chem., Int. Ed.*, 2017, **56**, 6431–6434.
20 I. Perez-Baena, I. Loinaz, D. Padro, I. Garcia, H. J. Grande and I. Odriozola, *J. Mater. Chem.*, 2010, **20**, 6916–6922.
21 G. Hariri, A. D. Edwards, T. B. Merrill, J. M. Greenbaum, A. E. van der Ende and E. Harth, *Mol. Pharm.*, 2014, **11**, 265–275.
22 Y. Bai, H. Xing, G. A. Vincil, J. Lee, E. J. Henderson, Y. Lu, N. G. Lemcoff and S. C. Zimmerman, *Chem. Sci.*, 2014, **5**, 2862–2868.
23 E. Huerta, P. J. M. Stals, E. W. Meijer and A. R. A. Palmans, *Angew. Chem., Int. Ed.*, 2013, **52**, 2906–2910.
24 I. Perez-Baena, F. Barroso-Bujans, U. Gasser, A. Arbe, A. J. Moreno, J. Colmenero and J. A. Pomposo, *ACS Macro Lett.*, 2013, **2**, 775–779.
25 A. Sanchez-Sanchez, A. Arbe, J. Colmenero and J. A. Pomposo, *ACS Macro Lett.*, 2014, **3**, 439–443.
26 Y. Bai, X. Feng, H. Xing, Y. Xu, B. K. Kim, N. Baig, T. Zhou, A. A. Gewirth, Y. Lu, E. Oldfield and S. C. Zimmerman, *J. Am. Chem. Soc.*, 2016, **138**, 11077–11080.
27 M. A. J. Gillissen, I. K. Voets, E. W. Meijer and A. R. A. Palmans, *Polym. Chem.*, 2012, **3**, 3166–3174.
28 A. Sanchez-Sanchez, S. Akbari, A. Etxeberria, A. Arbe, U. Gasser, A. J. Moreno, J. Colmenero and J. A. Pomposo, *ACS Macro Lett.*, 2013, **2**, 491–495.
29 A. Sanchez-Sanchez, S. Akbari, A. J. Moreno, F. L. Verso, A. Arbe, J. Colmenero and J. A. Pomposo, *Macromol. Rapid Commun.*, 2013, **34**, 1681–1686.
30 M. Huo, N. Wang, T. Fang, M. Sun, Y. Wei and J. Yuan, *Polymer*, 2015, **66**, A11–A21.
31 E. Harth, B. V. Horn, V. Y. Lee, D. S. Germack, C. P. Gonzales, R. D. Miller and C. J. Hawker, *J. Am. Chem. Soc.*, 2002, **124**, 8653–8660.
32 P. G. Frank, B. T. Tuten, A. Prasher, D. Chao and E. B. Berda, *Macromol. Rapid Commun.*, 2014, **35**, 249–253.
33 B. T. Tuten, D. Chao, C. K. Lyon and E. B. Berda, *Polym. Chem.*, 2012, **3**, 3068–3071.
34 A. Sanchez-Sanchez, D. A. Fulton and J. A. Pomposo, *Chem. Commun.*, 2014, **50**, 1871.
35 B. S. Murray and D. A. Fulton, *Macromolecules*, 2011, **44**, 7242–7252.
36 E. J. Foster, E. B. Berda and E. W. Meijer, *J. Am. Chem. Soc.*, 2009, **131**, 6964–6966.
37 E. B. Berda, E. J. Foster and E. W. Meijer, *Macromolecules*, 2010, **43**, 1430–1437.
38 N. Hosono, M. A. J. Gillissen, Y. Li, S. S. Sheiko, A. R. A. Palmans and E. W. Meijer, *J. Am. Chem. Soc.*, 2013, **135**, 501–510.
39 C. Boyer, N. A. Corrigan, K. Jung, D. Nguyen, T.-K. Nguyen, N. N. M. Adnan, S. Oliver, S. Shanmugam and J. Yeow, *Chem. Rev.*, 2016, **116**, 1803–1949.
40 A. Anastasaki, V. Nikolaou and D. M. Haddleton, *Polym. Chem.*, 2016, **7**, 1002–1026.
41 G. Moad, *Polym. Chem.*, 2017, **8**, 177–219.
42 G. Moad, E. Rizzardo and S. H. Thang, *Chem. – Asian J.*, 2013, **8**, 1634–1644.
43 J. Nicolas, Y. Guillaneuf, C. Lefay, D. Bertin, D. Gigmes and B. Charleux, *Prog. Polym. Sci.*, 2013, **38**, 63–235.
44 M. A. Gauthier, M. I. Gibson and H.-A. Klok, *Angew. Chem., Int. Ed.*, 2009, **48**, 48–58.
45 L. M. Campos, K. L. Killops, R. Sakai, J. M. J. Paulusse, D. Damiron, E. Drockenmuller, B. W. Messmore and C. J. Hawker, *Macromolecules*, 2008, **41**, 7063–7070.
46 F. Wang, B. Dong, H. Liu, J. Guo, W. Zheng, C. Zhang, L. Zhao, C. Bai, Y. Hu and X. Zhang, *Macromol. Chem. Phys.*, 2015, **216**, 321–328.
47 P. J. M. Stals, M. A. J. Gillissen, T. F. E. Paffen, T. F. A. de Greef, P. Lindner, E. W. Meijer, A. R. A. Palmans and I. K. Voets, *Macromolecules*, 2014, **47**, 2947–2954.
48 C. Cheng, K. Qi, D. S. Germack, E. Khoshdel and K. L. Wooley, *Adv. Mater.*, 2007, **19**, 2830–2835.
49 L. M. V. Renterghem, M. Lammens, B. Dervaux, P. Viville, R. Lazzaroni and F. E. D. Prez, *J. Am. Chem. Soc.*, 2008, **130**, 10802–10811.
50 B. V. K. J. Schmidt, N. Fechler, J. Falkenhagen and J.-F. Lutz, *Nat. Chem.*, 2011, **3**, 234–238.
51 J. Wen, J. Zhang, Y. Zhang, Y. Yang and H. Zhao, *Polym. Chem.*, 2014, **5**, 4032–4038.
52 W. Fan, X. Tong, Q. Yan, S. Fu and Y. Zhao, *Chem. Commun.*, 2014, **50**, 13492–13494.

53 E. J. Foster, E. B. Berda and E. W. Meijer, *J. Polym. Sci., Part A: Polym. Chem.*, 2011, **49**, 118–126.
54 F. Zhou, M. Xie and D. Chen, *Macromolecules*, 2014, **47**, 365–372.
55 G. Qian, B. Zhu, Y. Wang, S. Deng and A. Hu, *Macromol. Rapid Commun.*, 2012, **33**, 1393–1398.
56 J. A. Pomposo, J. Rubio-Cervilla, A. J. Moreno, F. Lo Verso, P. Bacova, A. Arbe and J. Colmenero, *Macromolecules*, 2017, **50**, 1732–1739.
57 L. Oria, R. Aguado, J. A. Pomposo and J. Colmenero, *Adv. Mater.*, 2010, **22**, 3038–3041.
58 A. R. de Luzuriaga, N. Ormategui, H. J. Grande, I. Odriozola, J. A. Pomposo and I. Loinaz, *Macromol. Rapid Commun.*, 2008, **29**, 1156–1160.
59 A. Sanchez-Sanchez, I. Asenjo-Sanz, L. Buruaga and J. A. Pomposo, *Macromol. Rapid Commun.*, 2012, **33**, 1262–1267.
60 I. Perez-Baena, I. Asenjo-Sanz, A. Arbe, A. J. Moreno, F. Lo Verso, J. Colmenero and J. A. Pomposo, *Macromolecules*, 2014, **47**, 8270–8280.
61 J. Jiang and S. Thayumanavan, *Macromolecules*, 2005, **38**, 5886–5891.
62 T. E. Dukette, M. E. Mackay, B. Van Horn, K. L. Wooley, E. Drockenmuller, M. Malkoch and C. J. Hawker, *Nano Lett.*, 2005, **5**, 1704–1709.
63 Y. Kim, J. Pyun, J. M. J. Fréchet, C. J. Hawker and C. W. Frank, *Langmuir*, 2005, **21**, 10444–10458.
64 A. Tuteja, M. E. Mackay, C. J. Hawker, B. Van Horn and D. L. Ho, *J. Polym. Sci., Part B: Polym. Phys.*, 2006, **44**, 1930–1947.
65 B. Zhu, J. Ma, Z. Li, J. Hou, X. Cheng, G. Qian, P. Liu and A. Hu, *J. Mater. Chem.*, 2011, **21**, 2679–2683.
66 B. Zhu, G. Qian, Y. Xiao, S. Deng, M. Wang and A. Hu, *J. Polym. Sci., Part A: Polym. Chem.*, 2011, **49**, 5330–5338.
67 O. Altintas, J. Willenbacher, K. N. R. Wuest, K. K. Oehlenschlaeger, P. Krolla-Sidenstein, H. Gliemann and C. Barner-Kowollik, *Macromolecules*, 2013, **46**, 8092–8101.
68 M. Glassner, K. K. Oehlenschlaeger, T. Gruendling and C. Barner-Kowollik, *Macromolecules*, 2011, **44**, 4681–4689.
69 F. Biedermann, E. A. Appel, J. S. del Barrio, T. Gruendling, C. Barner-Kowollik and O. A. Scherman, *Macromolecules*, 2011, **44**, 4828–4835.
70 H.-W. Engels, H.-G. Pirkl, R. Albers, R. W. Albach, J. Krause, A. Hoffmann, H. Casselmann and J. Dormish, *Angew. Chem., Int. Ed.*, 2013, **52**, 9422–9441.
71 J. D. Flores, J. Shin, C. E. Hoyle and C. L. McCormick, *Polym. Chem.*, 2010, **1**, 213–220.
72 N. Risangud, T. R. Congdon, D. J. Keddie, P. Wilson, K. Kempe and D. M. Haddleton, *J. Polym. Sci., Part A: Polym. Chem.*, 2016, **54**, 2698–2705.
73 J. B. Beck, K. L. Killops, T. Kang, K. Sivanandan, A. Bayles, M. E. Mackay, K. L. Wooley and C. J. Hawker, *Macromolecules*, 2009, **42**, 5629–5635.
74 S. Coca, C. B. Jasieczek, K. L. Beers and K. Matyjaszewski, *J. Polym. Sci., Part A: Polym. Chem.*, 1998, **36**, 1417–1424.
75 K. Bian and M. F. Cunningham, *Macromolecules*, 2005, **38**, 695–701.
76 L. Zhang, K. Katapodi, T. P. Davis, C. Barner-Kowollik and M. H. Stenzel, *J. Polym. Sci., Part A: Polym. Chem.*, 2006, **44**, 2177–2194.
77 X. Leng, N. H. Nguyen, B. van Beusekom, D. A. Wilson and V. Percec, *Polym. Chem.*, 2013, **4**, 2995–3004.
78 O. Wichterle and D. Lim, *Nature*, 1960, **185**, 117–118.
79 H. Kakwere and S. Perrier, *Polym. Chem.*, 2011, **2**, 270–288.
80 J. Zhang, G. Gody, M. Hartlieb, S. Catrouillet, J. Moffat and S. Perrier, *Macromolecules*, 2016, **49**, 8933–8942.
81 D. B. G. Williams and M. Lawton, *J. Org. Chem.*, 2010, **75**, 8351–8354.
82 V. Percec, T. Guliashvili, J. S. Ladislaw, A. Wistrand, A. Stjerndahl, M. J. Sienkowska, M. J. Monteiro and S. Sahoo, *J. Am. Chem. Soc.*, 2006, **128**, 14156–14165.
83 D. S. Tarbell, R. C. Mallatt and J. W. Wilson, *J. Am. Chem. Soc.*, 1942, **64**, 2229–2230.
84 X. Zhou, Y. Li, C. Fang, S. Li, Y. Cheng, W. Lei and X. Meng, *J. Mater. Sci. Technol.*, 2015, **31**, 708–722.
85 A. E. Cherian, F. C. Sun, S. S. Sheiko and G. W. Coates, *J. Am. Chem. Soc.*, 2007, **129**, 11350–11351.

